Longitudinal dispersion in natural channels: l. Experimental results from the River Severn, U.K.

T. C. Atkinson, P. M. Davis

Hydrology and Earth System Sciences, 4(3), *345–353* (2000) © EGS

Hydrology & Earth System Sciences

Longitudinal dispersion in natural channels: 1. Experimental results from the River Severn, U.K.

T.C. Atkinson[1,2] and P.M. Davis[2]

[1]Groundwater Tracing Unit, Department of Geological Sciences, University College London, London WC1E 6BT, U.K.
[2]School of Environmental Sciences, University of East Anglia, Norwich NR4 7TJ, U.K.
e-mail for corresponding author: t.atkinson@ucl.ac.uk

Abstract

A tracer experiment using Rhodamine WT dye was carried out to measure longitudinal dispersion in a 14-km reach of the River Severn in Wales, U.K. The river's discharge was measured at six points and the depth, width and cross-sectional area were measured at 86 points along the test reach. The channel geometry was close to being statistically uniform. Discharge and velocity were both nearly constant. Dye concentrations were recorded at stations between 210 and 13775 m downstream of injection. Dye was injected over a short interval as a near-uniform line source across the channel. These conditions make the data useful for testing mathematical theories of dispersion. They are presented in full.

Keywords: Channels; dispersion; tracers; River Severn

Introduction

The literature on the mechanics of tracer dispersion in natural channels is bedevilled by an abundance of theory and a lack of good, empirical data. This paper presents the results of a tracer experiment on the River Severn in Wales, U.K. Two sequel papers interpret the results in terms of dead zone dispersion models.

The theory of longitudinal dispersion by turbulent flow in pipes and conduits originates with a paper by Taylor (1954). He demonstrated theoretically the role of turbulent motion in producing a Fickian dispersion of tracer about the centre of a cloud which is advected along a channel at the same average velocity as the fluid, and presented an elegant series of laboratory experiments which appear to verify his theory. This has remained an important starting point for most discussions since. However, later laboratory and field experiments revealed that Taylor's predicted Gaussian distribution of tracer within an advecting cloud did not always occur (e.g. Glover, 1964; Fischer, 1967, 1968a, b; Sayre and Chang, 1968; Godfrey and Frederick, 1970; Thackston and Schnelle, 1970; Yotsukura *et al.*, 1970; Valentine and Wood, 1977, 1979a, b; Legrand-Marq and Laudelout, 1985). Actual clouds showed a marked asymmetry with the development over time of a pronounced tail. If the dispersion coefficient were estimated from the shape of the cloud as it passed a series of points downstream of an instantaneous release, its value appeared to increase with time and distance travelled (Godfrey and Frederick, 1970; Yotsukura *et al.*, 1970). Fischer (1968b) showed that Taylor's theory could account for the observed evolution of a tracer cloud only if it was applied to a series of short reaches, each being characterised by its own dispersion coefficient. Attempts to describe the whole evolution of a cloud by a single Taylorian dispersion coefficient were less successful.

The most rigorous test of a theory of longitudinal dispersion is its ability to describe the overall evolution of a cloud, not just the form of the cloud as it passes a single point on the channel. However, the literature of published field measurements contains few studies in which the form of a tracer cloud was recorded at more than one or two stations downstream of the point of release, whereas upwards of three stations are needed to discriminate the abilities of models to simulate cloud evolution with any rigour. A study of the Missouri River by Yotsukura *et al.* (1970) has been widely quoted, and compilations of data by Godfrey and Frederick (1970) and Nordin and Sabol (1974) contain a few more examples. All too often, where data on cloud evolution are available, the accompanying information on water discharge, channel dimensions and cross-sectional area is incomplete, so that the average properties of the channel cannot be established from the reported data. Many theories of dispersion subsequent to Taylor's (1954) depend upon assumptions which may be quite restrictive concerning the precise nature of the experimental set-up used to test them (for references see Davis *et al.*, 2000). For example it is common to assume that the channel is regular, straight, and

uniform and possesses constant average water velocity along its length, and that tracer is injected instantaneously as a uniform plane source. (Another class of theoretical treatments assume a point injection within a channel of finite width which is explicitly incorporated into equations. See for example Smith (1982), or Chatwin and Allen (1985) for a review.)

The work reported here originated through an interest in the possibility that dead zones might account for the non-Gaussian elements in the shapes of tracer clouds and their non-Fickian evolution. Davis *et al.* (2000) present the derivation of a mixed shear flow dispersion–dead zone model in which Taylor's (1954) theory is modified to take account of tracer exchange and storage in pockets of stationary and slow-moving water around the channel perimeter. This model assumes a regular, uniform channel in contact with uniform dead zones which are well mixed. Tracer may exchange by first-order diffusion between dead zones and the main channel. The model is one-dimensional, only longitudinal dispersion being considered. Average water velocity in the core channel is assumed constant along the river's length, and the tracer is assumed to originate from an instantaneous plane source. Thus, to test this model, experimental data were required from a natural channel with geometry that was as regular and uniform as possible, with steady and uniform flow, whose average water velocities and cross-sectional dimensions were known, and with a conservative tracer injected evenly across the whole cross-section. In 1978, an experiment was carried out to collect such data, using Rhodamine WT tracer in a 14 km long reach of the River Severn. The remainder of this paper describes the test reach and the conditions and results of the experiment.

Experimental conditions

THE TEST REACH

Two tracer dispersion tests were conducted on a 14 km long stretch of the River Severn in Britain (Fig. 1), between Llanidloes and Caersws. The tracer was injected at Llanidloes Bridge, and six sampling points (A-G) were located at distances between 210 m and 13775 m downstream. The exact locations of these points are given in Table 1. Most mathematical models of solute dispersion assume that the hydraulic conditions are time-invariant and uniform along the test reach. The River Severn at Llanidloes comes close to realising this ideal condition. In practice, few rivers in Britain show completely time-invariant discharge over the periods of hours to days needed to study longitudinal dispersion. However, the catchment of the Severn upstream of Station D is 187 km^2, which is large enough to supply a fairly steady baseflow. One

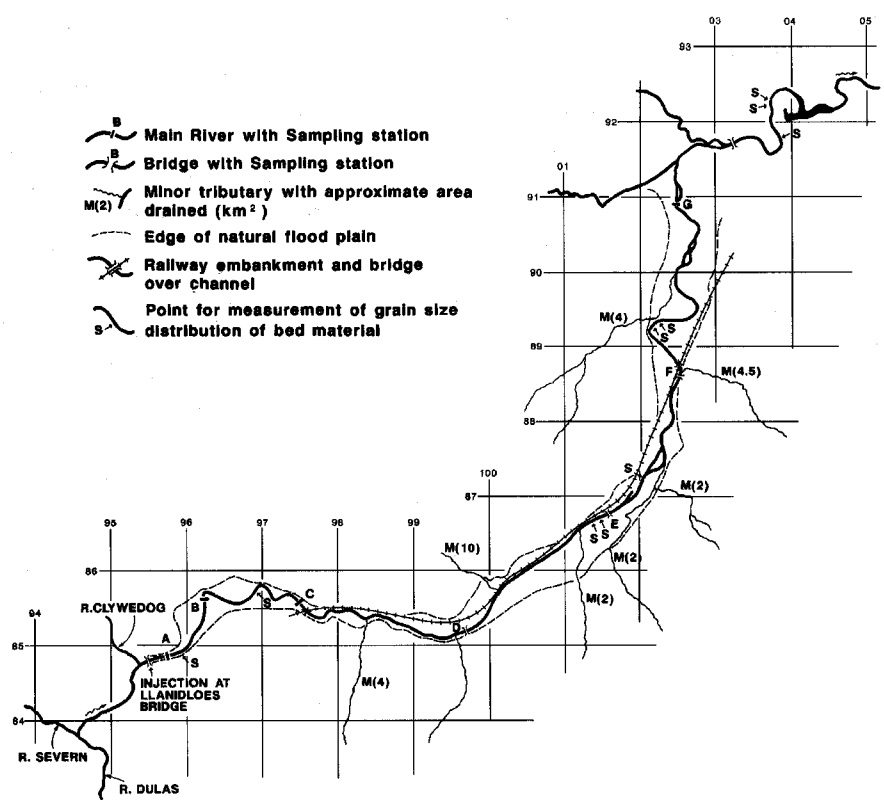

Fig. 1. *Map of the test reach on the River Severn downstream of Llanidloes, Powys, Wales, U.K. Grid is the 1-km National Grid, north at top.*

Table 1. Location of sampling points.

Site	Informal Name	U.K. National Grid Reference	Description	Distance (m)
Injection	Llanidloes Bridge	SN 9549 8479	3-arched bridge	0
A	Llanidloes Meadow	SN 9570 8488	left (north) bank, $^1/_3$ of width across channel	210
B	Dol-llys	SN 9621 8561	left bank, $^1/_4$ width, opposite field boundary	1175
C	Morfodion Ford	SN 9748 8558	100m downstream of ford, centre	2875
D	Dolwen	SN 9969 8518	upstream side of road bridge, centre	5275
E	Rickety Bridge	SO 0160 8677	beneath wooden foot bridge, centre	7775
F	Llandinam	SO 0252 8858	upstream side of road bridge, centre	10275
G	Carnedd	SO 0220 9090	right bank, opposite end of track	13775

of the major headwaters, the River Clywedog, is dammed to form a reservoir which was releasing a constant flow into the river at the time of the experiment. Thus, it was hoped that, if the experiment could be conducted in a period of settled weather, discharge would be approximately time-invariant. The test reach is the longest without important tributaries on the upper part of the River Severn. The valley is cut into low-permeability rocks, making it unlikely that groundwater inflows will increase the discharge significantly along the reach. These factors favour constancy of discharge along the test reach.

Constancy of hydraulic conditions requires that not only discharge but also channel dimensions be constant in a downstream direction. Few natural channels are uniform and the River Severn is no exception. In the test reach, the channel meanders in a flood plain which varies in width from less than 200 m to about one kilometre (Fig. 1). The width of the channel itself was measured at 86 points along the test reach (Fig. 2). It varies from 13 m to 48 m, averaging 24 m (mean width = 23.8 m, s.d. = 6.6 m). Figure 2 shows that the width along the channel varies considerably within distances of a few hundred metres.

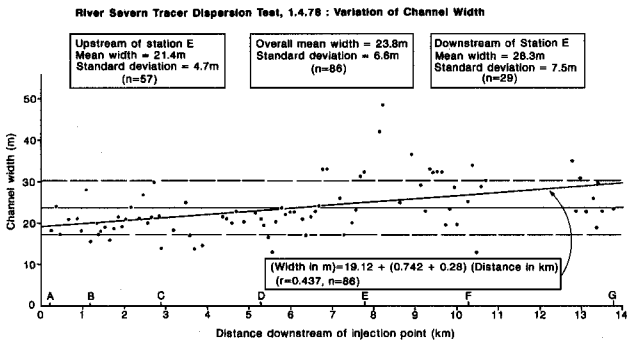

Fig. 2. *Variation of channel width as a function of distance. Overall mean width and standard deviations are shown as horizontal lines. The sloping line is the least-squares regression of width on distance.*

There is a slight, but significant tendency for width to increase in a downstream direction. Close inspection of the data suggests that this is not a steady increase, but rather that the channel changes in character somewhat at about the position of Station E (Fig. 2). Upstream of this point the channel tends to be narrower, with mean width 21.4 m (s.d. 4.7 m) while downstream it is wider, with a greater variability (mean width = 28.3 m, s.d. = 7.5 m). Figure 1 shows that the wider parts of the channel are associated with the more freely meandering part of the river where its flood plain broadens below Station E.

The depth of water was measured at 1 m intervals across each cross-section. Figure 3 shows average depth plotted against distance along the channel. Despite considerable variation over short distances, there is no trend in average depth along the test reach. The mean depth was 0.53 m, with a standard deviation of 0.18 m between sections.

The variation in depth occurs because the long profile of the river bed consists of a series of riffles and pools. The crests of the riffles are spaced several channel widths apart, with the pools forming deeper water between them. When in the field, it is difficult to perceive any obvious relationship between width and depth of the channel but there is a statistically significant correlation between them. Depth

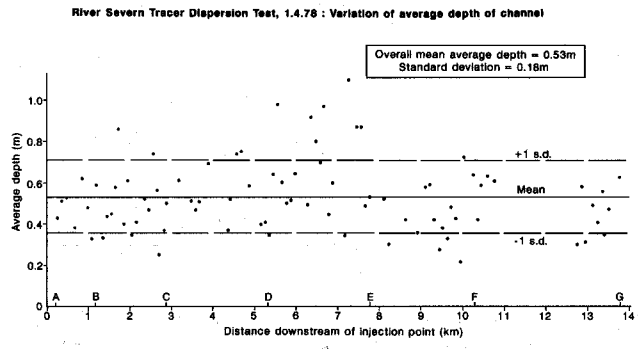

Fig. 3. *Variation of channel depth as a function of distance.*

tends to be less in wider channels. Linear regression gives the equation,

$$\underset{(m)}{(\text{Average depth})} = 0.81 - 0.012 \underset{(m)}{(\text{Width})} \qquad r = -0.43$$

It is important to note, however, that over 80% of the variance in depth is unexplained by changes in width. This variance is produced by the pool-and-riffle topography of the river bed.

Over almost all of the test reach, the channel is undivided. In two places there are short braided sections where the channel splits into two for a distance of one or two hundred metres. No cross-sections were measured in these short braided reaches, but the overall widths, average depths and total cross-sectional areas of the divided channels appeared similar to those of the normal, undivided parts.

The cross-sectional area was measured at 86 sections with the results shown in Fig. 4. There is a slight but statistically significant tendency for cross-sectional area to increase downstream, but as in the case of the width, this is not a steady increase. Rather, it is due to a relatively sudden increase in both average cross-sectional area and its variability at about 6.5 km downstream of the injection point. Below this the average cross-sectional area is 13.8 m^2 (s.d. = 4.1 m^2), while upstream it is 10.7 m^2 (s.d. = 2.8 m^2). This step change in cross-sectional area occurs a little upstream of the step change in width near Station E, because the channel between 6.5 km and Station E is mostly much deeper than average.

From these considerations of width, depth, and cross-sectional area it may be concluded that the channel shows variability on at least two scales. At the smallest scale that can be discriminated by these measurements, there is variability over distances of a few hundred metres. At a larger scale, there is evidence of downstream trends in width and cross-sectional area, but not in average depth. The channel is also more variable in the freely meandering reach downstream of Station E than it is above that point. The downstream trends are much weaker than the variability from section to section. Thus, the channel is certainly not uniform in the sense of being completely regular. However, it does appear to come as close to a condition of statistical uniformity as is likely to be found in any natural channel. Even so, it is not quite uniform even in a statistical sense, as there is evidence of a change in channel geometry around 6.5 to 7.8 km (Figs. 2 and 4) with significantly different means and standard deviations of width and area, above and below this region.

The material on the channel bed is coarse gravel composed of platy particles which have been winnowed clean of finer material within a surface layer roughly one particle thick. Below this the interstices of the gravel are filled with sand and mud. Under high flow conditions the bed is mobile, but there was no bed load transport of sediment during the experiments described here. Figure 5 shows the variation of particle size along the test reach. Although there is considerable variation in particle size from site to site, there is no evidence of any downstream trend.

DISCHARGE CONDITIONS AND MEASUREMENT

River discharge was measured at Stations A-F using standard current metering methods. Errors in individual estimates are likely in the region ±10%. Table 2, column 4, shows the results. The measurements were made during the first tracer test. Rain fell on high ground in the Severn headwaters during the day of the test and, by the time measurements were commenced at Stations E and F, the water level of the river had risen slightly. The increase in average depth at F was 2.5 cm, or 4%. The passage of a small flood wave from the headwater was probably responsible for the higher discharges recorded at E and F although some additional flow may have come from the small tributary streams which enter the main channel of the river from the valley sides along the test reach (Fig. 1). When the second test was conducted, the following day, the water level at Station F was steady at the same level as it had been during the current metering the previous day. Thus, there was an increase in discharge which took place during the first test. The peak of the dye cloud had passed Stations

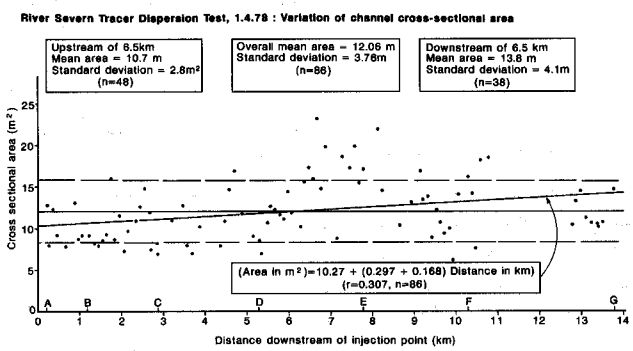

Fig. 4. *Variation of cross-sectional area as a function of distance. Horizontal lines show overall mean and standard deviations. Sloping line is the least-squares regression of cross-sectional area on distance.*

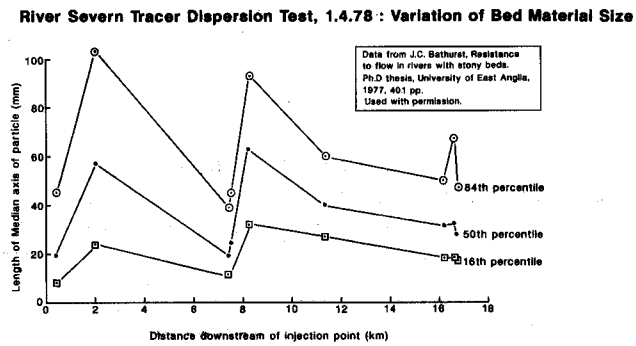

Fig. 5. *Variation of particle sizes in bed material as a function of distance.*

Table 2. Measured and calculated hydraulic parameters.

Station	Distance from injection (x) (m)	Local cross sectional area A_s (m^2)	Measured water discharge Q_s ($m^3.s^{-1}$)	Local velocity u_s ($m.s^{-1}$)	Upstream average cross section $\overline{A}_s$ (m^2)	Upstream average velocity $\overline{u}_s$ (ms^{-1})	Implied upstream discharge $\overline{Q}_s$ ($m^3 s^{-1}$)	Correction factor $\overline{Q}_s/Q_s$
A	210	10.62	7.33	0.69	10.54	0.69	7.27	0.99
B	1175	9.13	7.03	0.77	9.85	0.73	7.19	1.02
C	2875	10.81	7.24	0.67	10.07	0.71	7.15	0.99
D	5275	10.58	7.51	0.71	10.20	0.71	7.24	0.96
E	7775	22.56	9.25	0.41	11.76	0.65	7.64	0.83
F	10275	13.80	9.80	0.71	12.12	0.66	7.99	0.82
G	13775	–	(10)*	–	12.04	0.66	8.30	0.83

* Estimated value.

A to E before this increase took place, but the flood wave reached Station F at about the same time as the dye peak, and Station G a little before the dye peak. In the second test, discharge was steady at about the same value as had occurred during the flood wave the previous day. Though these fluctuations in discharge were easily measurable, it is shown below that they were not large enough to change the dispersion characteristics of the test reach significantly.

WATER VELOCITY IN THE TEST REACH

Table 2 shows the measured water discharge Q_s for each sampling station (except G which was not measured). From this and the cross-sectional area, the average water velocity can be found from,

$$u_s = \frac{Q_s}{A_s} \tag{1}$$

The subscript s indicates one of the stations A-G, as appropriate.

The movement of a tracer cloud is influenced by the average velocity in the whole length of channel which the cloud has traversed. To find this, a modification of (1) was first used to calculate a local velocity u_i at each of the 86 measured cross-sections,

$$u_i = \frac{Q_s}{A_i} \tag{1a}$$

with A_i the local cross-sectional area, and Q_s the measured discharge at the next current-metered station downstream of the locality under consideration. For each station A-G, an average upstream velocity $\overline{u}_s$ was then calculated from

$$\overline{u}_s = \frac{1}{n}\sum_{i=1}^{i=n} u_i \tag{2}$$

where n is the number of measured cross-sections upstream of the station (Table 2, column 7). The values show little variation, confirming the lack of overall trend in hydraulic conditions along the channel.

The average cross-sectional area upstream of a sampling station $\overline{A}_s$ is simply the mean of the n cross-sections lying upstream (Table 2, column 6). In analysing tracer dispersion data, some models may require upstream average values for both $\overline{A}_s$ and $\overline{u}_s$, which implies the existence of an "upstream average discharge" $\overline{Q}_s$ (Table 2, column 8),

$$\overline{Q}_s = \overline{A}_s.\overline{u}_s \tag{3}$$

THE TRACER TESTS: SAMPLING AND INJECTION PROCEDURES

Water samples were taken by hand, from about 10 cm below the surface, in glass vials which were stoppered and stored in a dark box for later analysis. Sampling intervals varied, depending on the location of the station. During the passage of the dye wave, the sampling interval was decreased to values which varied from 30 seconds at Station A to 10 minutes at F and 15 minutes at G.

The first experiment commenced at 10.36 on 1st April 1978 and lasted until 18.09 when the last sample was taken. Unfortunately, the dye cloud had not completely passed Station G at that time, so a second experiment was carried out on the following day, in which only F and G were sampled. Dye injection took place at 07.07 and the last samples were taken at 16.30.

In both experiments, the injection conditions were identical. Exactly 1000 gm of Rhodamine WT 20% solution supplied by the manufacturer was diluted to 5 litres volume with distilled water. The solution was injected beneath Llanidloes Bridge. The bridge has three arches and between the piers the river is about 30 cm deep. The dye solution was injected by a person walking steadily and briskly across the stream, immediately upstream of the bridge, and

pouring the dye from a 5-litre canister as he did so. Half the dye was injected on the outward journey and the other half on the return. This procedure distributed the dye evenly across the channel in the shortest possible time (105 seconds on 1st April, 109 seconds on 2nd April). Thus, the dye injection approximated, albeit crudely, to the line or plane source assumed in many analytical mathematical models from Taylor (1954) onwards.

Dye was analysed by fluorometry with a threshold of detectability of 0.1 parts per billion of the manufacturer's dye solution. Analytical errors were ±3% for concentrations greater than 10 ppb, rising to ±10% at 1 ppb and ±50% close to the detectable threshold. Since almost all of the dye was present in concentrations in excess of 1 ppb and most of the cloud had concentrations greater than 10 ppb, the contribution of analytical error to dye mass balance is probably ±4%.

Results

RAW DATA

The results of the tracer experiments are shown in Fig. 6 and the numerical values are presented in Table 3. In the first experiment, dye concentrations were measured at all the Stations A-G, but an incomplete record was obtained at G. In the second experiment, sampling was only carried out at Stations F and G. Thus, a comparison is possible between the two experiments for these two stations, and is shown graphically in Fig. 7. At Station E (Fig. 7a) the shape and concentrations of the dye clouds were almost identical on the two days except for a curious flat top to the peak on 1.4.78 (which may conceivably be due to misidentification of a sample during analysis). However, the slightly higher discharge conditions in the second experiment caused the dye cloud to migrate faster with an average time displacement between the two sets of 920 seconds. Thus, there was a 5% decrease in time of travel but little overall change in dispersion characteristics between the two experiments.

At Station G the comparison is not so complete (Fig. 7b) as only the first two-thirds of the dye cloud was recorded in the earlier experiment However, the second experiment again showed a faster time of travel with an average displacement of 640 seconds, representing a 2.8% decrease. In other respects, the sampled portions of the two curves are almost identical.

These comparisons demonstrate that the dispersive behaviour of the test reach is reproducible and that the cloud's velocity is more sensitive than its dispersion to small changes in discharge.

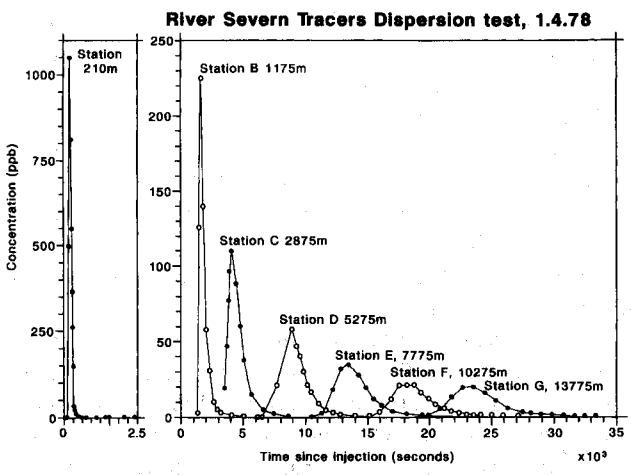

Fig. 6. *Combined results of the first and second tracer tests, shown as concentrations for each station plotted against time since injection. Expanded time scale shown for Station A.*

DATA REDUCTION

Completion of missing data

The data shown graphically in Fig. 6 are the raw results obtained in the first test, with the exception of the curve for Station G. For that station, the concentrations measured in the second test are used but the time since injection was adjusted to give the best fit with the velocity of the cloud recorded on the previous day. The adjusted points are shown graphically in Fig. 7, and their numerical values are shown in Table 3.

Table 3 thus comprises a consistent set of raw data for the discharge conditions measured in the first test.

Experimental errors and adjustment of concentrations to preserve mass balance

The mass of tracer present in the dye cloud as it passed each sampling point can be estimated from

$$m_s = Q_s \int_0^\infty c_s.dt \qquad (4)$$

where c_s is the dye concentration. The integral was found by 3-point parabolic interpolation between data points. The fractional recovery of tracer is m_s/M, where M is the mass injected. The mean of the first six values in Table 4 is 0.97 ± 0.048 (standard error) which does not differ significantly from unity, indicating that the dye cloud behaved conservatively.

The departure of individual values of fractional recovery from unity can be presumed to be due to experimental error (Table 4). The error involved in numerical integration was demonstrated to be negligible by integration of suitable known functions. The experimental error in concentrations was noted above to be around ±4%. This is also the minimum likely error in the integral in Eqn. (4). The likely error in current metering is ±10%. The combination of these errors (root sum of squares) yields an expected error in dye recovery of 11% which is commensurate with the

Table 3. Dye concentrations and sampling times.

Station A		Station B		Station C		Station D		Station E		Station F		Station G	
Time (secs)	Concen-tration (ppb)	Time (secs)	Concen-tration (ppb)	Time (secs)	Concen-tration (ppb)	Time (secs)	Concen-tration (ppb)	Time (secs)	Concen-tration (ppb)	Time (secs)	Concen-tration (secs)	Time (secs)	Concen-tration (ppb)
60	0.205	1320	3	3480	19.5	6480	0.21	10440	0.21	14220	0.1	17713	0.1
180	0.44	1440	126	3660	47	7680	21	11340	2.5	15120	0.43	18493	0.32
240	500	1560	225	3780	77	8880	58	12240	18	16020	4	19933	1.35
300	1050	1740	140	3900	96	9240	46.5	12840	32	16920	12	20833	4.7
330	810	1980	58	4020	110	9540	40	13440	34.5	17520	21	21733	13.5
360	550	2280	31	4140	110	9840	30	14280	28	18120	21	22633	19.5
390	365	2580	10	4440	88	10140	21	14880	19	18720	21	23533	20
420	260	2880	5	4740	60	10440	16.6	15480	12	19320	16	24433	16
450	147	3180	2.65	5040	38	11040	9	16080	8	19920	12	25333	11
540	32	4080	0.92	5640	15	11640	4.6	16980	4.1	20520	8.3	26233	5.9
570	26	4980	0.4	6540	4.8	12240	3	18180	2	21120	6.2	27373	3.3
600	19.5	6180	0.2	7440	2.2	12840	1.8	19380	1.1	21720	4.1	28033	2.3
630	11.7	7380	0.2	8640	0.38	14040	0.94	21180	0.66	22320	2.9	28933	1.6
660	8.1	8580	0.1	12360	0.1	15240	0.265	24000	0.43	22920	2.2	29833	1.25
690	5.4			13560	0.1	16440	0.21	25980	0.54	23520	1.7	30733	0.77
720	4.5			16560	0.32					24120	1.5	31633	0.43
780	2.3									25020	1.0	32533	0.43
840	1.5									25920	0.9	33433	0.43
900	1.4									27120	0.77		
1020	0.32												
1080	0.1												
1140	0.13												
1200	0.13												
1800	0.21												
1860	0.17												
1920	0.13												
2340	0.24												
2400	0.13												
3270	1.7												
3870	0.67												
4170	0.75												
4480	0.55												
5010	0.28												
5310	0.4												

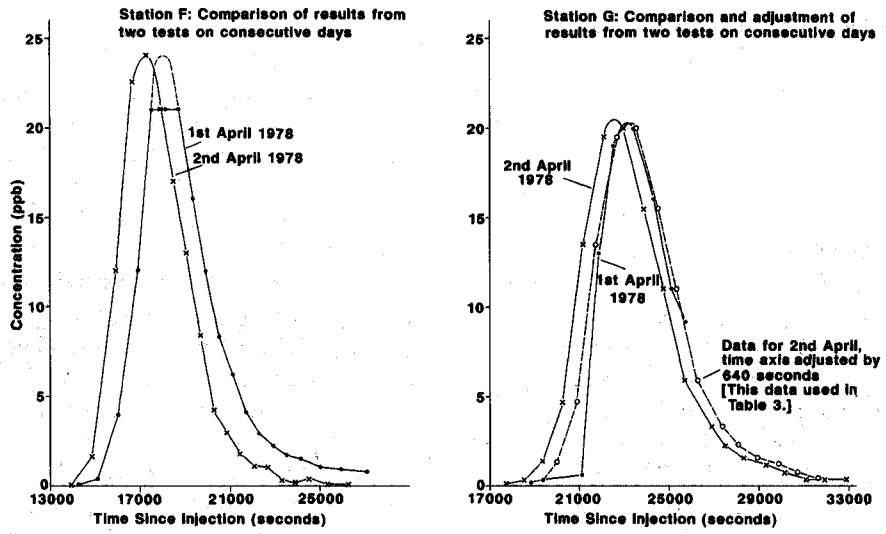

Fig. 7. *Comparison and adjustment of results from the first and second tests at Stations F and G.*

Table 4. Values of Fractional Recovery.

Station	m_s/M
A	1.079
B	0.784
C	1.026
D	0.990
E	1.067
F	0.868
G	(0.765)*
Mean+	0.969
s.d.+	0.118

* calculated using estimated local discharge of $10 m^3 s^{-1}$
\+ excludes values for G.

observed standard deviation (Table 4). Therefore it seems likely that the variability of values shown in Table 4 is entirely due to random experimental errors.

For purposes of comparing mathematical models of dispersion with data, the observed concentrations need to be corrected to the values they would have if dye mass balance was perfectly preserved without any experimental error. This can be achieved by dividing the observed concentrations in Table 3 by the corresponding fractional recoveries in Table 4.

Correction factor for variations in discharge and cross-sectional area along the test reach

In the companion papers to this one (Davis *et al.*, 2000; Davis and Atkinson, 2000) conditions upstream of a station are specified in the form of the average cross-sectional area and average velocity ($\overline{A}_s$ and $\overline{u}_s$). As noted above, these figures imply an "upstream average discharge" given by their product (Eqn. (3) and Table 2, column 8). Since these values are not the same as the local discharges used to calculate mass balance (Q_s Table 2, col. 4), a further adjustment of concentrations is necessary to preserve the theoretical mass balance in fitted models. This correction factor is shown in Table 2, column 9.

It is important to note that this last adjustment factor arises from the specific type of model to be fitted to the data, and the way in which measured parameter values are specified for use in it. Therefore, it is philosophically more appropriate to adjust the model output by a factor necessary to preserve mass balance consistency with the measured data, rather than the other way around. In fitting models to the data in Table 3, the model output has been multiplied by the correction factors shown in column 9 of Table 2 (Davis *et al.*, 2000; Davis and Atkinson, 2000). Readers wishing to use this data to test models of their own are urged to derive their own adjustment factors which are appropriate to the circumstances.

Discussion and conclusions

The data presented in Tables 3 and 4 together describe the evolution of a conservative tracer cloud along the test reach of the River Severn. Taken together with the hydraulic data in Table 2, they provide a set of empirical observations which can be used to test a wide variety of models of the longitudinal dispersion processes in a natural river. The test reach was chosen for its near conformity to constant discharge and regularity of width, depth, cross-sectional area, and bed material size. While these dimensions do vary considerably over short distances, there are minimal downstream trends in the test reach and the average water velocity is almost constant over distances of hundreds to thousands of metres. Thus, the hydraulic conditions conform as closely as possible to the uniform velocity and cross-sectional area assumed in many mathematical treatments of dispersion.

The calculated fractional recoveries indicate the essentially conservative behaviour of Rhodamine WT as a tracer in surface waters, at least under the conditions of negligible suspended load and coarse bed sediments which obtained in the River Severn. However, experimental errors in mass balance of up to 15% can be expected using the methods and instruments employed here.

The function of this paper is to present the data of Tables 2, 3 and 4, in the hope that future analysts and modellers may find it useful in studying the complex mix of processes involved in tracer dispersion in natural channels. An analysis of the data is presented in terms of longitudinal dispersion by turbulence and exchange with dead zones in two companion papers (Davis *et al.*, 2000; Davis and Atkinson, 2000).

List of Symbols

A_i	measured cross-sectional area at location i
A_s	measured cross-sectional area at a station s
$\overline{A}_s$	average cross-sectional area upstream of a station s
c_s	measured tracer concentration at a station s
i	(subscript) one of the 86 locations where width, depth and cross-sectional area were measured
m_s	mass of tracer recovered experimentally passing a station s
M	measured mass of tracer injected
Q_s	measured river discharge at a station s
$\overline{Q}_s$	average discharge upstream of a station s
s	(subscript) one of the current-metering and tracer sampling locations A-G
u_i	cross-sectional average water velocity at location i
u_s	cross-sectional average water velocity at a station s
$\overline{u}_s$	average water velocity upstream of a station s

Acknowledgements

John Trillwood, Duncan Tamsett and other students assisted with data collection. Phil Judge drew the diagrams. P.M. Davis was supported by a Natural Environment Research Council Training Award.

References

Chatwin, P.C. and Allen, C.M., 1985. Mathematical models of dispersion in rivers and estuaries. *Annu. Rev. Fluid Mech.*, **17**, 119–149.

Davis, P.M., Atkinson, T.C. and Wigley, T.M.L., 2000. Longitudinal dispersion in natural channels 2: The roles of shear-flow dispersion and dead zones in the River Severn, U.K. *Hydrol. Earth System Sci.*, **4**, 355–371.

Davis, P.M. and Atkinson, T.C., 2000. Longitudinal dispersion in natural channels 3: An aggregated dead zone model applied to the River Severn, U.K. *Hydrol. Earth System Sci.*, **4**, 373–381.

Fischer, H.B., 1967. The mechanics of dispersion in natural streams. *J. Hydraul. Div. A.S.C.E.*, **93**, 187–216.

Fischer, H.B., 1968a. Methods for predicting dispersion coefficients in natural streams, with applications to lower reaches of the Green and Duwamish Rivers. *U.S. Geological Survey Professional Paper*, **582A**.

Fischer, H.B., 1968b. Dispersion predictions in natural streams. *J. Sanitary Engng. A.S.C.E.*, **94**, 927–943.

Glover, R.E., 1964. Dispersion of dissolved or suspended materials in flowing streams, *U.S. Geological Survey Professional Paper*, **433B**.

Godfrey, R.G. and Frederick, B.J., 1970. Stream dispersion at selected sites. *U.S. Geological Survey Professional Paper*, **433K**.

Legrand-Marcq, C. and Laudelout, H., 1985. Longitudinal dispersion in a forest stream. *J. Hydrol.*, **78**, 317–324.

Nordin, C.F. and Sabol, G.V., 1974. Empirical data on longitudinal dispersion in rivers. *U.S. Geological Survey, Water Resources Investigations*, **20–74**.

Sayre, W.W. and Chang, F.M., 1968. A laboratory investigation of open-channel dispersion processes for dissolved, suspended and floating dispersants. *U.S. Geological Survey Professional Paper*, **433E**.

Smith, R., 1982. Gaussian approximations for contaminant dispersion. *Quart. J. Mech. Appl Math*, **35**, 345–366.

Taylor, G.I., 1954. The dispersion of matter in turbulent flow through a pipe. *Proc. Roy. Soc. London, Ser.* **A**, **223**, 446–468.

Thackston, E.C. and Schnelle, K.B., 1970. Predicting effects of dead zones on stream mixing. *J. Sanitary Engng. Div. A.S.C.E.*, **96**, 319–331.

Valentine, E.M. and Wood, I.R., 1977. Longitudinal dispersion with dead zones. *J. Hydraul. Div. A.S.C.E.*, **103**, 975–990.

Valentine, E.M. and Wood, I.R., 1979a. Experiments in longitudinal dispersion with dead zones. *J. Hydraul. Div. A.S.C.E.*, **105**, 999–1016.

Valentine, E.M. and Wood, I.R., 1979b. Dispersion in rough rectangular channels. *J. Hydraul. Div. A.S.C.E*, **105**, 1537–1553.

Yotsukura, N., Fischer, H.B. and Sayre, W.W., 1970. Measurement of mixing characteristics of the Missouri River between Sioux City, Iowa, and Plattsmouth, Nebraska. *U.S. Geological Survey Water-Supply Paper*, **1899-G**.